Proceedings of the ASME 2024 43rd International Conference on Ocean, Offshore and Arctic Engineering
OMAE2024
June 9-14, 2024, Singapore, Singapore

OMAE2024-131914

VIBRATION AND FATIGUE MITIGATION OF A 5 MW BARGE-TYPE FLOATING OFFSHORE WIND TURBINE UNDER MISALIGNED WIND AND WAVE LOADINGS

Riad El hamoud[1], Philip Alkhoury[2], Mourad Aït-Ahmed[3], Abdul-Hamid Soubra[1], Franck Schoefs[1], Rabih Dib[4]

[1]Nantes Université, École Centrale Nantes, CNRS, GeM, UMR 6183, IUML, FR 3473, F-44600 Saint-Nazaire, France
[2]Formerly Nantes Université, École Centrale Nantes, CNRS, GeM, UMR 6183, IUML, FR 3473, F-44600 Saint-Nazaire, France
[3]Nantes Université, Institut de Recherche en Énergie Électrique de Nantes Atlantique, IREENA, UR 4642, IUML, FR CNRS 3473, F-44600 Saint-Nazaire, France
[4]LaRGES, Faculty of Engineering, Lebanese University, Tripoli, Lebanon

ABSTRACT

This paper aims at investigating vibration suppression and fatigue mitigation of a 5 MW barge-type floating offshore wind turbine (FOWT) under misaligned wind and wave loadings. A passive omnidirectional tuned mass damper (TMD) installed in the floating platform was employed. The aero-hydro–servo-elastic coupled simulation program for wind turbines, OpenFAST, was used to perform the numerical simulations. The omnidirectional TMD was tuned to the platform pitch and roll natural frequencies in order to mitigate the vibration and fatigue loads in fore-aft and side-side directions respectively. The TMD damping ratios in fore-aft and side-side directions were obtained from two minimization procedures where the objective functions are the standard deviations of platform pitch and platform roll motion respectively. The effectiveness of the omnidirectional TMD was checked for one load case under three misalignment angles $(0°\,;45°\,;90°)$. *The percentage change of the standard deviation (SD) and damage equivalent moment (DEM) between the controlled and the uncontrolled cases were used as indicators of vibration suppression and fatigue mitigation respectively. The obtained results have shown that the omnidirectional TMD can effectively mitigate vibrations and fatigue of the FOWT under misaligned wind and wave loadings. For instance, the reduction in SD of platform pitch and DEM of tower base fore-aft moment could attain 47% and 31% respectively in the case of a misalignment angle between wind and wave of* $90°$. *Moreover, a comparison with an equivalent dual TMD was carried out. It was found that the omnidirectional TMD provides better bi-directional vibration and fatigue mitigation when compared to the dual TMD.*

Keywords: FOWT; Barge platform; Vibration; Damage equivalent moment; misaligned wind and wave loadings; omnidirectional TMD; OpenFAST

1. INTRODUCTION

In our world today, sustainable energy demand grows exponentially. The need of energy sources is important and more particular the renewable sources of energy. Among these sources, wind energy will play a key role [1]. The trend to wind energy is being led by the European Union with a total installed offshore wind capacity of 19.1 GW in 2022 [1]. The dominant substructures in offshore wind farms are bottom-fixed including monopiles, jackets and gravity base foundations [1]. These types of wind turbines are installed in shallow water, for a depth between 30~50 m. However, in deep water, the wind is steadier and less turbulent which constitutes a more favorable condition for wind turbines than ones installed near shore. Installing bottom-fixed wind turbines in deeper water is not competitive to reach the Levelized Cost of Energy [2]. Here comes the idea of Floating Offshore Wind Turbine (FOWT). FOWTs are subjected to harsh stochastic wind and wave loadings. Furthermore, they are dynamically sensitive structures to wind and wave excitations. This leads to the severe vibrations of the FOWT tower and platform. Such severe vibrations may cause failure or even defunction under the fatigue induced loads. Indeed, these severe vibrations cause repetitive moments at some critical points (e.g. tower base) which could lead to a fatigue failure. To reduce the dynamic responses (displacements and damage equivalent loads DEL) of the FOWT under wind and wave excitations, two main control strategies are used: the pitch-angle control strategy and the application of structural control devices. The pitch control strategy lies in changing the aerodynamic characteristics of the rotor to reduce the dynamic response. However, this leads to an excessive usage of the blade pitch actuator causing fatigue at the blade root. Further, this control strategy will not work when the wind speed is lower than cut-in and higher than cut-off [3]. The application of structural control devices has been investigated and proven to be effective in reducing the dynamic responses of the structures including FOWT [4]. This strategy consists of attaching a device to the primary structure to absorb the kinetic energy and thus to reduce the dynamic response. There are three types of structural control strategies: passive, semi-active and active. Semi-active and active control strategies require energy input. In contrast, passive TMD which stands for Tuned Mass Damper does not require external energy and it is widely used in offshore wind turbines for dynamic response mitigation.

In this paper, the aim is to reduce (i) the rotational vibration of the platform (pitch and roll), (ii) the translational vibration of the tower top displacement in fore-aft and side-side directions, (iii) the fatigue loads at tower base and at blade root, in both fore-aft and side-side directions. Note that the different degrees of freedom (DoF) of the platform and tower of the FOWT may be seen in Figure 1b.

Different authors have considered vibration reduction of FOWTs. For instance, Yang and He [5] established a multi-degree of freedom (MDOF) model for a 5 MW spar-type FOWT. Genetic algorithm was used to minimize the standard deviations of platform pitch and tower top displacement in fore-aft direction based on a pitch free decay test, the objective being the determination of the optimal parameters of two TMDs placed in the nacelle and the platform. Han et al. [6] established a MDOF model for a 5 MW semi-submersible FOWT. As in Yang and He [5], two TMDs were used and the optimal TMDs parameters were obtained based on a pitch free decay test making use of a genetic algorithm. Notice however that a single objective function was used by these authors. This objective function involves the standard deviation of tower top fore-aft displacement. Jin et al. [7] established a MDOF model of a 5 MW barge-type FOWT in order to find the optimal parameters of two TMDs placed in the nacelle and the platform. The artificial fish swarm algorithm (AFSA) was used to obtain the TMDs optimal parameters based on a pitch free decay test. The objective function used by these authors was the standard deviation of the tower top fore-aft displacement as in Han et al. [6]. Han et al. [8] established a MDOF model of a 5 MW barge-type FOWT with a tuned liquid column damper (TLCD) inside the barge platform. An exhaustive search process was used to obtain the optimal parameters of the TLCD. As in Han et al. [6] and Jin et al. [7], the optimal parameters of the TLCD were obtained based on a pitch free decay test and the objective function was the standard deviation of tower top fore-aft displacement.

All the above-mentioned studies found the optimal parameters of the TMD/TLCD using a free decay test. However, an optimization in free decay test is far from a realistic representation of the ocean conditions in which dynamic and stochastic loads are applied to wind turbine structures. Instead of using a free decay test to optimize TMD parameters, some authors make use of real conditions of wind and wave. Indeed, Park et al. [9] established a MDOF model for a 5 MW spar-type FOWT and used a bilinear TMD placed in the platform to mitigate platform pitch motion. The parameters of the bilinear TMD were optimized using a genetic algorithm under a stochastic wind speed and by setting the standard deviation of platform pitch as the objective function to minimize. Notice however that the strategy used by Park et al. [9] makes use of a single realization of wind speed. There is no guarantee that the obtained parameters remain optimal for another realization. In addition to the above-mentioned shortcoming, all the above-mentioned studies have not considered the misalignment between wind and wave.

In this paper, a passive omnidirectional TMD that considers the effect of wind and wave misalignment is used. Realistic wind and wave loadings were considered. Three scenarios that cover the three regimes of the FOWT were adopted. A novel methodology based on the PSDs (Power Spectral Density) of the FOWT displacements and fatigue loads is employed to find the frequency of the omnidirectional TMD and the free decay test is used to find the damping ratio of this TMD. The PSDs-based method is more robust than the method adopted by Park et al. [9] which uses a single realization of wind to tune the TMD.

The research content in this paper is organized as follows: In Section 2, a dynamic analysis of the 5 MW barge-type FOWT is carried out. Section 3 presents the proposed new methodology to tune the omnidirectional TMD. In section 4, the proposed methodology is applied and the optimal TMD parameters are obtained. In section 5, a comparison with a dual TMD is carried out. Finally, section 6 presents the conclusion.

2. DYNAMIC ANALYSIS OF THE 5 MW BARGE-TYPE FOWT

2.1 Definition of the 5 MW barge-type FOWT

In this paper, the 5 MW barge-type FOWT developed by the National Renewable Energy Laboratory (NREL) was investigated for vibration and fatigue analyses. The wind turbine is a conventional three-bladed, upwind, variable speed, and blade-pitch-angle-controlled turbine [10]. A barge-type foundation developed by ITI Energy [11] was selected as the floating-support structure. The barge platform is a squared shape platform and it has a catenary mooring system consisting of eight lines, where two lines emanate from each corner of the platform. The main parameters of the 5 MW barge-type FOWT are given in [11] and a schematic is shown in Figure 1a.

2.2 Natural frequencies of the 5 MW barge-type FOWT

An eigenanalysis of the 5 MW barge-type FOWT was performed in this section based on free decay tests using OpenFAST v3.5 [12]. Notice that a free decay test for a given mode consists in applying an initial displacement of say 1 m (or an initial angle of say 1°) in the absence of wind and wave loadings. The PSDs of the obtained time series are then computed. For each PSD, the frequency which corresponds to the maximum power is the natural frequency of the corresponding mode. The natural frequencies obtained in this paper were compared with those provided by Matha et al. [13] in Table 1. The last column gives the relative difference in percent.

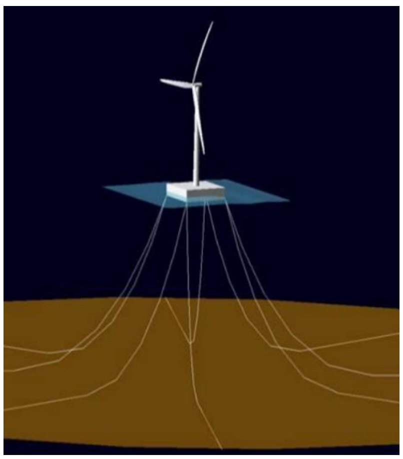

Figure 1a: Illustration of the NREL 5 MW barge-type FOWT [8]

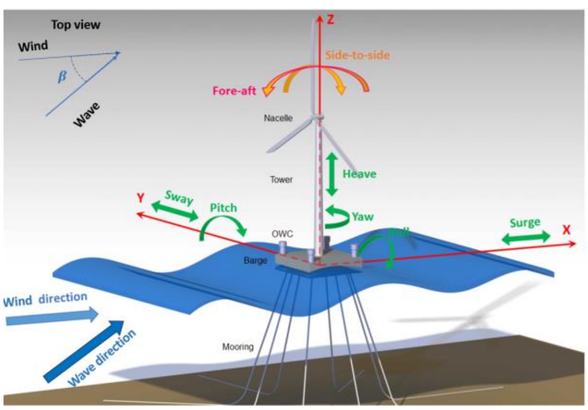

Figure 1b: Illustration of platform and tower DoFs

According to Table 1, significant discrepancies were obtained for (i) platform surge, (ii) platform sway, (iii) platform heave, (iv) platform yaw and (v) tower 1st bending mode in side-side direction. However, small discrepancies were found for platform roll, platform pitch and tower 1st bending mode in fore-aft direction. Since, the objective of the paper is to reduce (i) vibration of platform roll and pitch, (ii) tower top displacement in both fore-aft and side-side directions (iii) fatigue at tower base in both fore-aft and side-side directions and (iv) fatigue at blade root moment, the degrees of freedom which show important discrepancies (except that of the tower 1st bending mode in side-side direction) are not important in this study because their effect is limited to the fatigue of mooring lines. This topic is out of the scope of this paper. The discrepancy in tower 1st bending mode in side-side direction may be explained by the fact that in Matha [13], the generator Degree of Freedom (DoF) was not activated during the free decay test (result not shown in this paper).

3. METHODOLOGY USED TO TUNE THE OMNIDIRECTIONAL TMD

An omnidirectional TMD was used in this paper. This TMD consists of a single mass with two pairs of springs and dashpots placed in fore-aft and side-side directions. It may move in both fore-aft and side-side directions with a planar motion. The methodology proposed in this paper to tune the omnidirectional TMD consists in finding the following four parameters of this TMD: (i) the natural angular frequency in fore-aft direction ω_x, (ii) the natural angular frequency in side-side direction ω_y, (iii) the damping ratio in fore-aft direction ζ_x and (iv) the damping ratio in side-side direction ζ_y. This methodology includes two steps:

(a) In the first step, one determines the natural angular frequencies ω_x and ω_y in fore-aft and side-side directions respectively. The natural angular frequency ω_x was made equal to the platform pitch natural angular frequency. This is because (i) the platform pitch, (ii) the tower top displacement in fore-aft direction, (iii) the tower base moment in fore-aft direction and (iv) the blade root moment in flapwise direction, were found in this paper to be all excited by the platform pitch frequency as will be shown later in section 3.1. Indeed, the PSDs of the above-mentioned outputs exhibit maximum power at a common frequency which is found equal to the platform pitch frequency. Similarly, the natural angular frequency ω_y was made equal to the platform roll natural angular frequency because (i) the platform roll, (ii) the tower top displacement in side-side direction and (iii) the tower base moment in side-side direction, were also found in this paper to be all excited by a common frequency that is equal to the platform roll frequency. Note that PSD of blade root moment in edgewise direction has zero power at the platform roll frequency which means that a TMD tuned to platform roll frequency will not reduce the blade root moment in edgewise direction.

(b) In the second step, one determines the damping ratios ζ_x and ζ_y in fore-aft and side-side directions respectively. A free decay test of the platform pitch (respectively platform roll) was used to find the optimal damping ratio ζ_x (respectively ζ_y) in the fore-aft (respectively side-side) direction. Indeed, for each free decay test, damping ratios ranging from 0.01 to 1 were tested. The optimal damping ratio $\zeta_{optimal,x}$ (respectively $\zeta_{optimal,y}$) in fore-aft direction (respectively in side-side direction) is defined as the damping ratio that minimizes the standard deviation of platform pitch (respectively platform roll).

The proposed methodology is quite robust for the two following reasons:

(a) The natural angular frequencies ω_x and ω_y used in this paper for the tuning of the omnidirectional TMD in both the fore-aft and the side-side directions were obtained from a spectral analysis making use of the PSDs of the different output signals. Notice that the PSD of a given output signal (displacement or fatigue load) is unique for the ensemble of possible stochastic realizations of this output in the time domain. Therefore, tuning the omnidirectional TMD based on the PSD guarantees a reduction of the FOWT response for all possible realizations of this output.

(b) To find the optimal damping ratio $\zeta_{optimal,x}$ (respectively $\zeta_{optimal,y}$) in fore-aft (respectively side-side) direction, a minimization procedure leading to an optimal value of the damping coefficient was employed. The objective function used was the standard deviation of the platform pitch (respectively platform roll) signal as obtained from a platform pitch (respectively platform roll) free decay test.

Mode	Natural frequency (Hz) by the present paper	Natural frequency (Hz) by Matha [9]	Discrepancy (%)
Platform surge	0.0069	0.0076	−10.14
Platform sway	0.0069	0.0076	−10.14
Platform heave	0.136	0.1283	6
Platform roll	0.0842	0.0854	−1.42
Platform pitch	0.0836	0.0849	−1.53
Platform yaw	0.0183	0.0198	−7.57
Tower 1st bending mode in fore-aft direction	0.5249	0.5282	−0.62
Tower 1st bending mode in side-side direction	0.5896	0.5375	9.69

Table 1: Comparison of the natural frequencies of the 5 MW barge-type FOWT

3.1 Identification of the excited modes for use in the tuning of the omnidirectional TMD

In order to identify the excited modes to be used in the tuning of the omnidirectional TMD, the PSDs of (i) platform roll and pitch, (ii) tower top displacement in fore-aft and side-side directions, (iii) tower base moment in fore-aft and side-side directions and (iv) blade root moment in flapwise and edgewise directions, were computed. Three simulation scenarios (cf. Table 2) were used to cover the three regimes of the wind turbine (below rated, rated and above rated regimes). In the three scenarios, the wind speed field is assumed to be stochastic and it was generated using Kaimal spectrum. The wave elevation field is also assumed to be stochastic and it was generated using JONSWAP spectrum. Moreover, in the three scenarios, the wind and wave are assumed to be aligned. Notice that the values of the wind speed presented in Table 2 are consistent with the design of the FOWT. Indeed, the 5MW rotor has (i) a cut-in wind speed of $3\ m/s$ (ii) a rated wind speed of $11.4\ m/s$ and (iii) a cut-off wind speed of $25\ m/s$ [10]. The rotor is parked when the wind speed is (i) lower than cut-in wind speed (i.e. $3\ m/s$) or (ii) greater than cut-off wind speed (i.e. $25\ m/s$).

The below rated regime is defined for any wind speed between the cut-in and rated wind speed (here chosen as 8 m/s). The rated regime comprises any wind speed between the rated and cut-off wind speed (here chosen as 12 m/s). In this regime, the FOWT produces its rated power (i.e. 5 MW herein). The above rated regime is defined for any wind speed higher than cut-off (here chosen as 37 m/s). Notice that the three sea-states considered in Table 2 have a peak period T_p of 12.5 s in order to obtain a corresponding frequency ($f_p = \frac{1}{T_p} = \frac{1}{12.5} = 0.08\ Hz$) that is close to platform pitch and roll frequencies, the objective being to excite these two modes by the wave loading. It should be noted that for the three scenarios (and also when calculating the natural frequencies of the FOWT), no TMD was added to the FOWT.

	Wind speed (V)	Significant wave height (H_s)	Peak period (T_p)	Regime
Scenario 1	8 m/s	2 m	12.5 s	Below rated
Scenario 2	12 m/s	2.6 m	12.5 s	Rated
Scenario 3	37 m/s	7 m	12.5 s	Above rated

Table 2: Three simulation scenarios used to compute PSD

Figures 2-5 show the PSDs of the displacements and loads in the fore-aft direction and Figures 6-8 show the PSDs of the same outputs in the side-side direction except the one of the blade root moment in edgewise direction which was found not to be excited neither by the wind nor by the wave. Due to paper length limitation, only PSDs obtained based on Scenario 1 are provided, the PSDs due to Scenarios 2 and 3 being of similar trends.

The PSDs of displacements and loads in fore-aft direction (cf. Figures $2-5$) show a peak with the highest power at a common frequency which is equal or nearly equal to the platform pitch frequency ($f = 0.0849\ Hz$). Some PSDs show another peak with a smaller power at a frequency which is nearly equal to the tower 1st bending mode in fore-aft direction ($f = 0.5282\ Hz$). Similarly, the PSDs of displacements and loads in side-side direction (cf. Figures $6-8$) show a peak with the highest power at a common frequency which is equal or nearly equal to the platform roll frequency ($f = 0.0854\ Hz$).

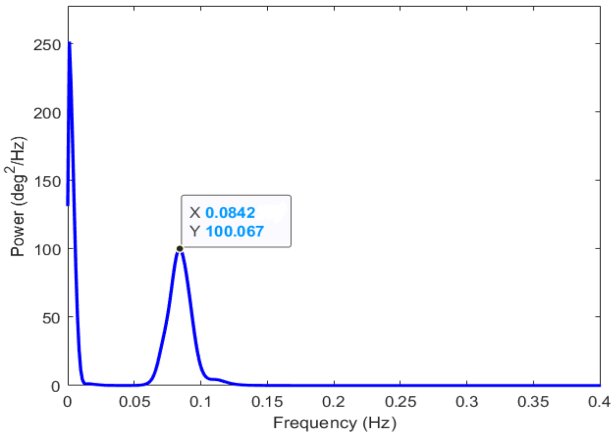

Figure 2: PSD of platform pitch

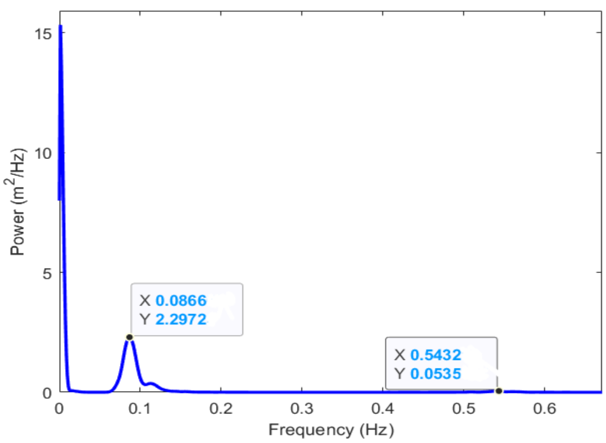

Figure 3: PSD of tower top fore-aft displacement

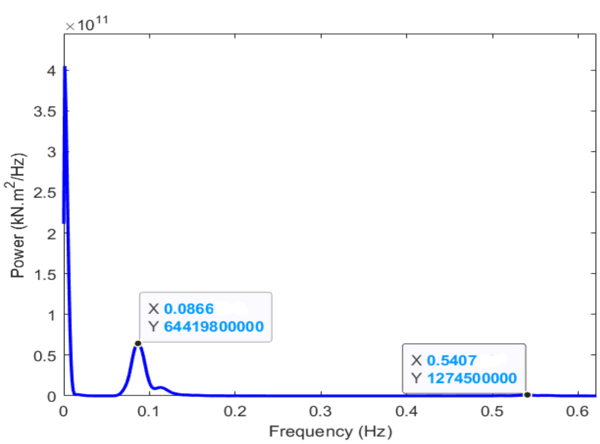

Figure 4: PSD of tower base fore-aft moment

Some PSDs show another peak with a smaller power at a frequency which is equal or nearly equal to the tower 1st bending mode in side-side direction ($f = 0.5896Hz$).

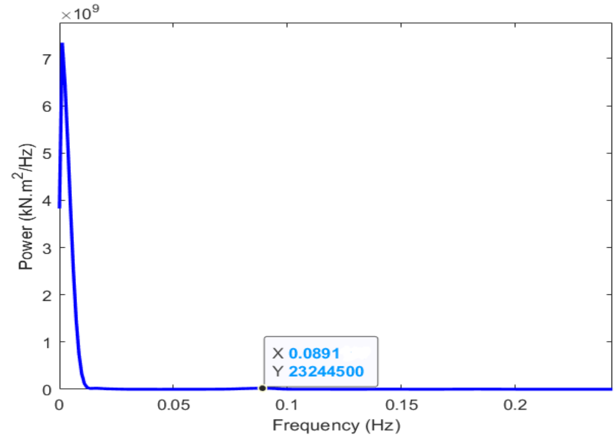

Figure 5: PSD of blade root moment in flapwise direction

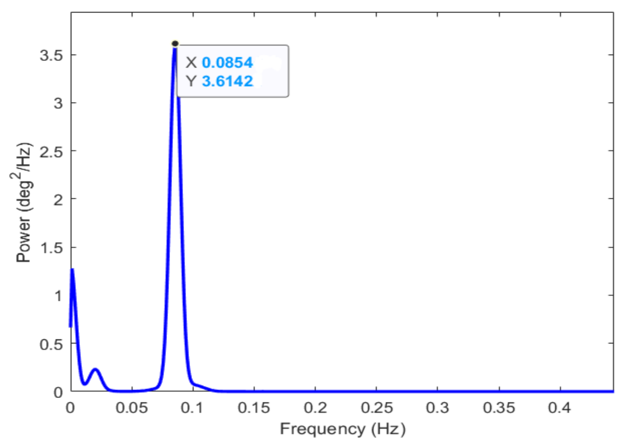

Figure 6: PSD of platform roll

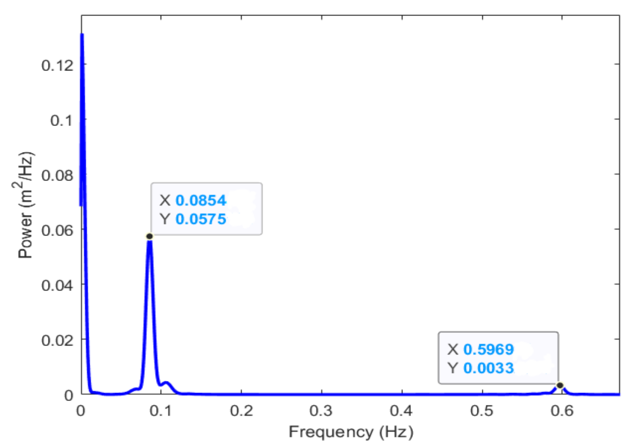

Figure 7: PSD of tower top side-side displacement

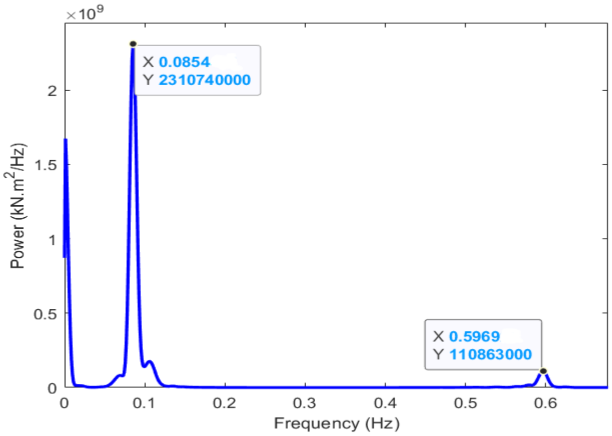

Figure 8: PSD of tower base side-side moment

To conclude, the FOWT responses in fore-aft direction (platform pitch, tower top displacement in fore-aft direction, tower base moment in fore-aft direction and blade root moment in flapwise direction) show the highest power at platform pitch frequency for the three scenarios that cover the three regimes of the FOWT. Thus, a TMD tuned to the platform pitch frequency could mitigate the vibrations (platform pitch and tower top displacement in fore-aft direction) and fatigue in fore-aft direction (tower base moment in fore-aft direction and blade root moment in flapwise direction). On the other hand, the FOWT responses in side-side direction (platform roll, tower top displacement in side-side direction, tower base moment in side-side direction), show the highest power at platform roll frequency for the three scenarios that cover the three regimes of the FOWT. Thus, a TMD tuned to the platform roll frequency could mitigate the vibrations (platform roll and tower top displacement in side-side direction) and fatigue in side-side direction (tower base moment in side-side direction).

4. OPTIMAL PARAMETERS OF AN OMNIDIRECTIONAL TMD

4.1 Calibration of the omnidirectional TMD

This section presents the first step of the methodology adopted in this paper to tune the omnidirectional TMD. According to the previous section where the PSDs of the different outputs have shown the highest power at platform pitch and platform roll frequencies, the omnidirectional TMD should be tuned to platform pitch frequency and to platform roll frequency in order to mitigate (i) fatigue at tower base in fore-aft and side-side directions and at blade root in flapwise direction and (ii) vibrations in fore-aft direction (platform pitch and tower top fore-aft displacement) and side-side direction (platform roll and tower top side-side displacement).

Due to the fact that the platform pitch mode and the platform roll mode are the most excited modes (i.e., the modes with the highest power for the three regimes of the FOWT-see section 3.1), an omnidirectional TMD that may move in both the fore-aft and the side-side directions would be beneficial to mitigate vibration and fatigue in both directions (i.e., fore-aft and side-side directions) under misaligned wind and wave loadings. Note that adding a TMD slightly changes the natural frequencies of the FOWT.

According to [5-7,9,14], a TMD should have a mass ratio lower than 5%. Therefore, the omnidirectional TMD is chosen to have a mass, M, corresponding to 5% of the overall mass of the FOWT, i.e. $M = 307473\ kg$. This mass is considered in order to obtain maximum mitigation effect. The TMD is added at the bottom of the barge platform i.e. at $-4\ m$ under the mean sea level. The omnidirectional TMD has two pairs of springs and dashpots. The first pair is placed in fore-aft direction while the other pair is placed in side-side direction. The springs stiffness of the omnidirectional TMD in fore-aft and side-side directions are denoted k_x and k_y respectively. The damping coefficients of the omnidirectional TMD in fore-aft and side-side directions are denoted c_x and c_y respectively.

The natural angular frequency ω_x of the omnidirectional TMD in the fore-aft direction is related to its spring stiffness k_x in the fore-aft direction and its mass M by the following equation (similar relationship remains valid for the side-side direction):

$$k_x = M \times (\omega_x)^2 \quad (1)$$

The damping coefficient c_x of the omnidirectional TMD in the fore-aft direction is related to the damping ratio ζ_x in the fore-aft direction, the TMD mass M and its natural angular frequency ω_x as follows (similar relationship remains valid for the side-side direction):

$$c_x = 2 \times M \times \omega_x \times \zeta_x \quad (2)$$

4.2 Optimal damping ratios of the omnidirectional TMD

This section presents the second step of the proposed methodology which aims at finding the optimal damping ratio $\zeta_{optimal,x}$ (respectively $\zeta_{optimal,y}$) in fore-aft (respectively side-side) direction. To find the optimal damping ratio $\zeta_{optimal,x}$ (respectively $\zeta_{optimal,y}$) in fore-aft (respectively side-side) direction, a free decay test of platform pitch (respectively platform roll) was used. This test consists in applying an initial pitch angle (respectively roll angle) at time $t = 0$ in the absence of wind and wave. In our method, the omnidirectional TMD (which is tuned to the platform pitch in fore-aft direction and platform roll in side-side direction) was added to the platform while performing the two free decay tests.

Figure 9 shows the standard deviation of platform pitch and platform roll for different damping ratios ranging from 0.01 to 1. From this figure, one could notice that both the standard deviation of platform pitch and the standard deviation of platform roll exhibit a minimum at a given value of the damping ratio (which will be called hereafter optimal value of the damping ratio). Furthermore, this value of damping ratio was found quasi-identical in both directions where $\zeta_{optimal,x} \approx \zeta_{optimal,y} = 0.08$. The quasi-equality of the damping ratios in both x and y directions is expected because the natural frequencies of platform roll and pitch are very close.

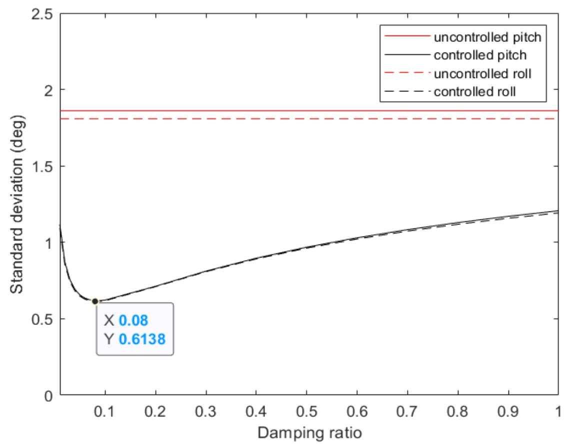

Figure 9: Variation of the standard deviation of platform pitch (solid curve) and roll (dashed-curve) versus the damping ratio of the omnidirectional TMD

A comparison of the platform pitch time series and its PSD was carried out between the three following cases (i) the uncontrolled case (ii) the controlled case where the damping ratio ζ is set to the optimal value (i.e. $\zeta = 8\%$) and (iii) the controlled case where the damping ratio ζ is set to two arbitrary values of 4% and 20%. The comparisons were performed for three initial values of platform pitch $(2° ; 5° ; 8°)$. Figure 10 shows the platform pitch time series for the three cases considering different values of the damping ratio and for the uncontrolled case.

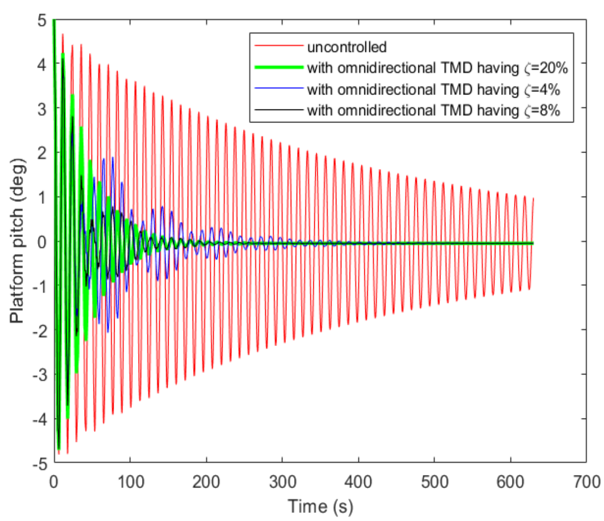

Figure 10: Comparison of the free decay test of platform pitch for the (i) uncontrolled case (ii) controlled case with ζ = 8% (iii) controlled case with the two arbitrary values ζ = 4% and ζ = 20% when the initial platform pitch is 5°

Figure 11 shows their corresponding PSDs. An initial platform pitch of 5° was taken in these figures. The results of the two other initial values of platform pitch (i.e. 2° & 8°), were not provided herein as they exhibit similar trend.

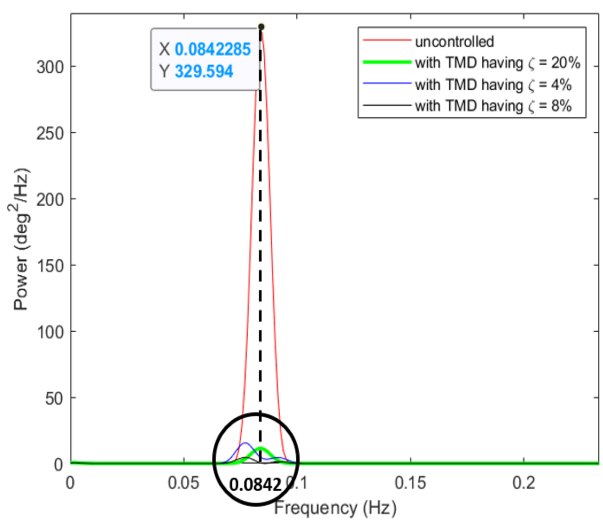

Figure 11: Comparison of the PSD of the free decay test of platform pitch for the (i) uncontrolled case (ii) controlled case with ζ = 8% (iii) controlled case with the two arbitrary values of ζ (ζ = 4% and ζ = 20%) when the initial platform pitch is 5°

Figure 12 shows a zoom of the area limited by the thick black circle in Figure 11.

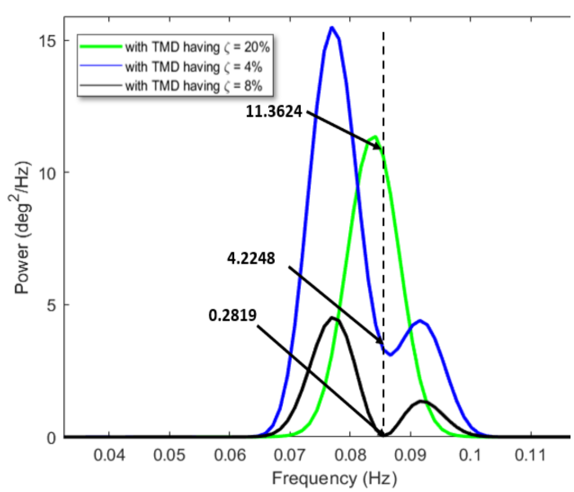

Figure 12: Zoom of the curves that appear inside the thick black circle in Figure 11

According to Figure 12, it is clear that the omnidirectional TMD having the optimal damping ratio of $\zeta = 8\%$ (see black curve) leads to a quasi-vanishing power as compared to the two other cases with the arbitrary values of ζ $(\zeta = 0.04 ; 0.2)$ [see blue and green curves]. Notice that the relationship between the variance σ^2 of a signal in time domain and its corresponding PSD is given by the following equation:

$$\sigma^2 = \frac{1}{2\pi}\int_{-\infty}^{+\infty} S(\omega)\, d\omega \qquad (3)$$

where σ is the standard deviation of the signal and $S(\omega)$ is its PSD. According to Equation (3), the variance is proportional to the area underneath the PSD. As it can be seen from Figure 12, the area underneath the PSD where $\zeta = 0.08$ (black curve) is much smaller than the one (red curve) of the uncontrolled case. This reduction of the area which means a reduction in SD [Equation (3)] confirms the result of the optimization of the standard deviation performed above. Similar result (not shown in this paper) was obtained for platform roll.

Notice that the maximum power of all the treated cases $(\zeta = 0.04\,;0.08\,;0.2)$ is associated to a frequency of 0.0842 Hz which is close to platform pitch frequency ($f^{platform\ pitch} = 0.0849\,Hz$). As may be seen from Figure 12, the power associated to the frequency of platform pitch is respectively equal to $11.3624\,;4.2248$ and 0.2819 deg^2/Hz for $\zeta = 0.2\,;\ 0.04$ and 0.08 confirming the fact that a minimal power was obtained for the optimal damping ratio of 0.08.

Table 3 shows the optimal parameters (k_x, k_y, c_x, c_y) of the omnidirectional TMD as obtained using the methodology proposed in this paper.

Mass	Stiffness	Damping
$M = 307473\,kg$	$k_x = 87495\,N/m$	$c_x = 26243\,N.s/m$
	$k_y = 88528\,N/m$	$c_y = 26398\,N.s/m$

Table 3 : Parameters of the Omnidirectional TMD

To conclude, the omnidirectional TMD which has a mass of 5% of the overall mass of the FOWT should be tuned to platform pitch in fore-aft direction and platform roll in side-side direction. For the two directions, the optimal damping ratio obtained was equal to 8% $(\zeta_{optimal,x} \approx \zeta_{optimal,y} \approx 0.08)$.

5. COMPARISON BETWEEN THE OMNIDIRECTIONAL TMD AND THE EQUIVALENT DUAL TMD

This section aims at comparing the fatigue and vibration mitigation as obtained using the omnidirectional TMD and the equivalent dual linear independent TMDs. The dual TMD is composed of two TMDs that move in two orthogonal directions. The two TMDs have a total mass equal to the mass of the omnidirectional TMD i.e., 5% of the overall mass of the FOWT. Five mass distributions between the two orthogonal TMDs are considered: (i) (100% FA - 0% SS), (ii) (66% FA - 33% SS), (iii) (50% FA - 50% SS), (iv) (33% FA - 66% SS) and (v) (0% FA - 100% SS). For instance, (66% FA - 33% SS) is equivalent to say that 66% of the omnidirectional TMD mass is placed in fore-aft direction and 33% of this omnidirectional TMD mass is placed in side-side direction. The unidirectional TMD placed in fore-aft (respectively side-side) direction has a mass m_{FA} (respectively m_{SS}), a damping ratio ζ_{FA} (respectively ζ_{SS}) of 8%, a spring stiffness k_{FA} (respectively k_{SS}), a damping coefficient c_{FA} (respectively c_{SS}). It is tuned to platform pitch frequency and platform roll frequency using Equations (1) and (2). Table 4 shows orthogonal TMDs parameters for the five mass distributions. The 5 MW barge-type FOWT was simulated under one load case in rated regime. This load case is defined by a mean wind speed of 18 m/s and a sea state defined by $H_s = 4\,m$ and $T_p = 12.5\,s$. Three misalignment angles $(\beta = 0°\,;45°\,;90°)$ between wind and wave were considered. Note that for each misalignment angle, only one seed (i.e. a unique realization) was simulated. To evaluate the effect of the omnidirectional TMD and the dual TMD on vibration reduction, standard deviation of platform pitch and roll and standard deviation of tower top displacement in fore-aft and side-side directions were computed.

		Mass (kg)	Stiffness (N/m)	Damping $(N.s/m)$
100% FA - 0% SS	TMD in fore-aft direction	$m_{FA} = 307473$	$k_{FA} = 87494$	$c_{FA} = 26243$
	TMD in side-side direction	$m_{SS} = 0$	$k_{SS} = 0$	$c_{SS} = 0$
66% FA - 33% SS	TMD in fore-aft direction	$m_{FA} = 204777$	$k_{FA} = 58271$	$c_{FA} = 17478$
	TMD in side-side direction	$m_{SS} = 102696$	$k_{SS} = 29568$	$c_{SS} = 8817$
50% FA - 50% SS	TMD in fore-aft direction	$m_{FA} = 153736$	$k_{FA} = 43747$	$c_{FA} = 13121$
	TMD in side-side direction	$m_{SS} = 153736$	$k_{SS} = 44264.2$	$c_{SS} = 13199$
33% FA - 66% SS	TMD in fore-aft direction	$m_{FA} = 102696$	$k_{FA} = 29223$	$c_{FA} = 8765$
	TMD in side-side direction	$m_{SS} = 204777$	$k_{SS} = 58960$	$c_{SS} = 17581$
0% FA - 100% SS	TMD in fore-aft direction	$m_{FA} = 0$	$k_{FA} = 0$	$c_{FA} = 0$
	TMD in side-side direction	$m_{SS} = 307473$	$k_{SS} = 88528$	$c_{SS} = 26398$

Table 4: Parameters of the orthogonal TMDs

Concerning the effect of the omnidirectional TMD and the dual TMD on fatigue mitigation at tower base and blade root, short-term damage equivalent moment (DEM) was computed. Notice that the different simulations of the different cases considered in this paper have a duration of $630\,s$ and when computing STD and DEM, the first 30 seconds were disregarded in order not to take into account the transient time. Note finally that a DEM is a constant amplitude moment that occurs at a fixed moment mean and frequency and produces the same equivalent damage as the stochastic time series. The moment mean value considered herein is set to zero. According to [14], the expression of the DEM is given in Equation (4) as follows:

$$DEM = \left(\frac{\sum_i [n_i (M_i)^m]}{f^{eq} \times T}\right)^{\frac{1}{m}} \quad (4)$$

Where, (i) n_i and M_i are the number of cycles and the moment range for i-th load reversal respectively, (ii) m is Wohler exponent (iii) f^{eq} is the DEM frequency and (iv) T is the duration of the time-series. In wind turbine application, $f^{eq} = 1\ Hz$.

To compute DEM at tower base and blade root, rainflow counting algorithm and SN curve were adopted. For the tower base (respectively blade root), the Wohler exponent used was 3 (respectively 10) (see [8]). The relative difference is used as an indicator of improvement in comparison with the uncontrolled case. The expressions of the relative difference for standard deviation and the relative difference for DEM are given respectively in equations (5) and (6) as follows:

$$\eta_\sigma = \frac{\sigma^{uncontrolled} - \sigma^{controlled}}{\sigma^{uncontrolled}} \quad (5)$$

$$\eta_{DEM} = \frac{DEM^{uncontrolled} - DEM^{controlled}}{DEM^{uncontrolled}} \quad (6)$$

In order to see the effect of the omnidirectional TMD and the dual TMD on vibration and fatigue mitigation for three misalignment angles, Figures 13-15 show the improvement of (i) DEM of tower base moment in fore-aft and side-side directions, (ii) DEM for blade root moment in flapwise direction (iii) STD of platform pitch and roll and (iv) STD of tower top displacement in fore-aft and side-side directions, for three wind wave misalignment angles ($\beta = 0°\,;45°\,;90°$).

According to Figure 13 where $\beta = 0°$, one could notice that the omnidirectional TMD provides better bi-directional fatigue and vibration mitigation than the ensemble configurations of the dual TMD. Indeed, the omnidirectional TMD shows the highest reductions for both displacements and loads in fore-aft and side-side directions. The maximum reduction is obtained in the standard deviation of the platform roll where the reduction attains 45%.

According to Figures 14 and 15 where β is equal to 45° and 90° respectively, one could notice that the omnidirectional TMD provides the same reduction in displacements and loads in side-side direction as the 0% FA - 100% SS configuration of the dual TMD. However, the superiority of the omnidirectional TMD appears in its capability to achieve more reduction in displacement and fatigue in fore-aft direction as compared to 0% FA - 100% SS. For instance, when $\beta = 45°$, the reduction by the omnidirectional TMD can attain 39% for platform roll and 20% for platform pitch versus a reduction of 38% for platform roll and 5% for platform pitch as compared to the 0% FA - 100% SS configuration of the dual TMD. On the other hand, when $\beta = 90°$, the reduction by the omnidirectional TMD can attain (i) 40% for platform roll (ii) 47% for platform pitch and (iii) 31% for DEM at tower base in fore-aft direction versus a reduction of (i) 40% for platform roll (ii) 40% for platform pitch and (iii) 23% for DEM at tower base in fore-aft direction by the 0% FA - 100% SS configuration of the dual TMD. As a conclusion, the superiority of the omnidirectional TMD lies in the fact that it could achieve the highest reduction in both fore-aft and side-side directions at the same time.

It should be noted that stroke limiters were used in all the numerical simulations. They are arbitrarily placed in this paper at $\pm\ 18\ m$ (smaller than $\pm\ 20\ m$ which represent the borderlines of the platform) from the center of this platform in order to let a safe distance between the position of the stroke limiter and the boundaries of the platform.

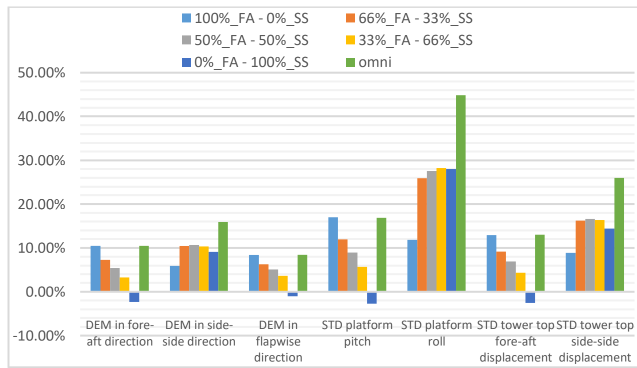

Figure 13: Percentage improvement for $\beta = 0°$

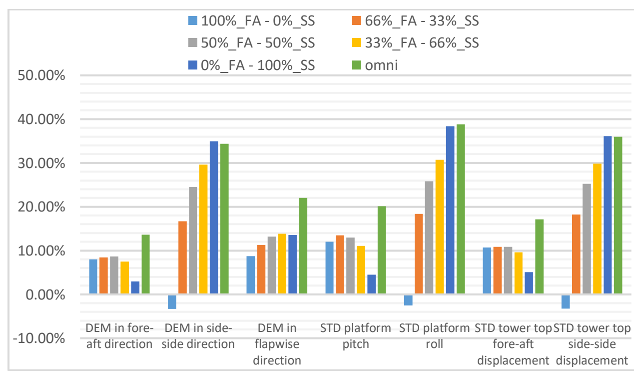

Figure 14: Percentage improvement for $\beta = 45°$

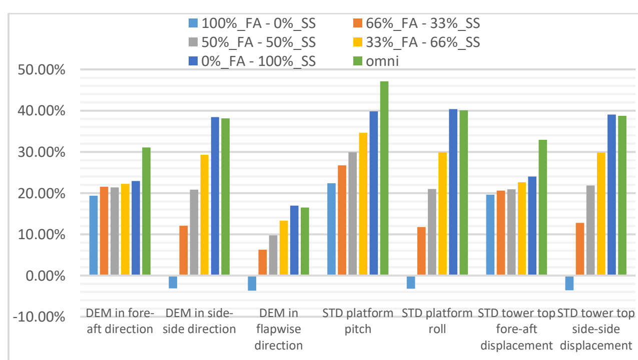

Figure 15: Percentage improvement for $\beta = 90°$

In the literature, there are no specific guidelines for stroke limiters stiffness and damping coefficients. The values of stiffness and damping coefficients for the stroke limiters given by Han et al. [6] and Si et al. [15] are respectively ($k_{stop,x} = 5 \times 10^5 \ N/m$ and $c_{stop,x} = 5 \times 10^5 \ N.s/m$) and ($k_{stop,x} = 1 \times 10^6 \ N/m$ and $c_{stop,x} = 5 \times 10^6 \ N.s/m$).
The stiffness and damping coefficients for the stroke limiters as adopted herein were $k_{stop,x} = k_{stop,y} = 5 \times 10^7 \ N/m$; $c_{stop,x} = c_{stop,y} = 5 \times 10^7 \ N.s/m$. By using these values, the stroke of the omnidirectional TMD was found not to exceed the platform limits as shown in Figure 16.

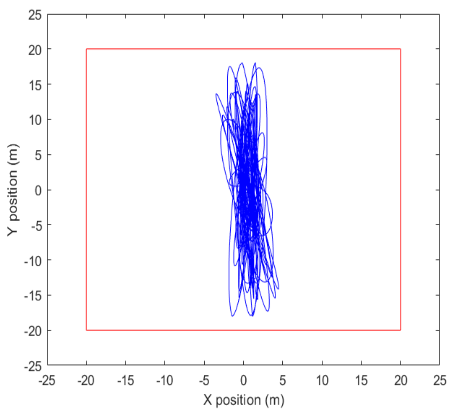

Figure 16: Omnidirectional TMD trajectory in the barge platform when $\beta = 90°$ and when the stroke limiters are added

6. CONCLUSION

In this paper, a passive omnidirectional TMD was used to reduce vibrations and fatigue (in both fore-aft and side-side directions) of a 5 MW barge-type FOWT under misaligned wind and wave loadings. In order to tune the omnidirectional TMD, the natural angular frequencies in fore-aft and side-side directions were obtained from a spectral analysis of the FOWT outputs performed in both fore-aft and side-side directions. Indeed, the omnidirectional TMD placed in the platform and tuned to platform pitch frequency (respectively platform roll frequency) was used to mitigate vibration and fatigue loads in fore-aft (respectively in side-side) direction. The damping ratios in fore-aft and side-side directions were obtained from minimization procedures of the platform rotational motion (the standard deviation of platform pitch and roll) as obtained from free decay tests. A comparison between the omnidirectional TMD and the equivalent dual TMD was performed. Results have shown that the omnidirectional TMD provides better bi-directional vibration and fatigue mitigation when compared to the equivalent dual TMD.

ACKNOWLEDGEMENTS

This work was carried out within the framework of the WEAMEC, West Atlantic Marine Energy Community, and the funding from CARENE and *Région Pays de la Loire*.

REFERENCES

[1] https://windeurope.org/intelligence-platform/product/wind-energy-in-europe-2022-statistics-and-the-outlook-for-2023-2027/
[2] Musial, W., Butterfield, S., Ram, B., 2006. Energy from offshore wind. In: Offshore Technology Conference, pp. 1888–1898.
[3] Lackner, M.A., Rotea, M.A., 2011. Passive structural control of offshore wind turbines. Wind Energy 14 (3), 373–388.
[4] Soong, T.T., Costantinou, M.C., 2014. Passive and active structural vibration control in civil engineering. Springer.
[5] Yang, J.J., He, E.M., 2020. Coupled modeling and structural vibration control for floating offshore wind turbine. Renewable Energy 15,678694.
[6] Han, D., Wang, W., Li, X., Su, X., 2022. Optimization design of multiple tuned mass dampers for semi-submersible floating wind turbine. Ocean Engineering 264, 112536.
[7] Jin, X., Xie, S., He, J., Lin, Y., Wang, Y., Wang, N., 2018. Optimization of tuned mass damper parameters for floating wind turbines by using the artificial fish swarm algorithm. Ocean Engineering 167, 130-141.
[8] Han, D., Li, X., Wang, W., Su, X., 2023. Dynamic modeling and vibration control of barge offshore wind turbine using tuned liquid column damper in floating platform. Ocean Engineering 276,114299.
[9] Park, G., Oh, K.-Y., Nam, W., 2022. Bilinear tuned mass damper for spar-type floating wind turbines. Ocean Engineering 261, 112081.
[10] Jonkman, J., Butterfield, S., Musial, W., Scott, G., 2009. Definition of a 5-MW reference wind turbine for offshore system development (No. NREL/TP-500-38060, 947422).
[11] Jonkman, J.M., 2007. Dynamics modeling and loads analysis of an offshore floating wind turbine (No. NREL/TP-500-41958, 921803).
[12] OpenFAST Documentation, 2022. Release v3.1.0. National Renewable Energy Laboratory. Code published at. https://github.com/OpenFAST/openfast. https://openfast.readthedocs.io/en/master/.
[13] Matha, D., 2010. Model development and loads analysis of an offshore wind turbine on a tension leg platform with a comparison to other floating turbine concepts: April 2009.
[14] MLife Theory Manual for Version 1.00.
[15] Si, Y., Karimi, H.R., Gao, H., 2014. Modelling and optimization of a passive structural control design for a spar-type floating wind turbine. Engineering Structures 69, 168–182.